Electron backscattering diffraction study of coalesced bainite in high strength steel weld metals

E. Keehan*[1], L. Karlsson[2], H. K. D. H. Bhadeshia[3] and M. Thuvander[2]

Coalesced bainite is a coarse constituent recently found to develop along with the classical martensite, lower and upper bainite in steel weld metals. Its crystallography has been characterised using electron backscattering diffraction in combination with field emission gun scanning electron microscopy. It is confirmed that coalesced bainite grains are crystallographically homogeneous but do contain orientation gradients. The misorientations across different grains of coalesced bainite and relative to conventional bainite have also been studied. The observations are discussed in the context of the mechanism by which coalesced bainite evolves.

Keywords: Coalesced Bainite, EBSD, FEGSEM, High strength steel weld metals

Introduction

Developing steel weld metals stronger than ~690 MPa (100 ksi) which are also tough continue to be a challenge in spite of some 50 years of research on the subject.[1–3] At these strength levels, the weld metal microstructure is a mixture of bainite and martensite with their relative proportions determining the mechanical properties.

Conventional weld metal microstructures, consisting of allotriomorphic, Widmanstätten and acicular ferrite can be resolved using light optical microscopy (LOM). However, bainite and martensite plates have some dimensions less than the wavelength of light, making it difficult to characterise using LOM, or even conventional scanning electron microscopy (SEM).[4] Transmission electron microscopy (TEM) has the limitation that minute regions are examined, making it difficult to get an overall view. On the other hand, field emission gun scanning electron microscopy (FEGSEM) offers both high resolution (~nm) and a large field of view so that the feature observed can be placed in context.[4] When FEGSEM is combined with electron back scattered diffraction (EBSD), morphological observations can be supplemented with crystallographic information.[5]

Using FEGSEM, a microstructure previously not reported in steel weld metals – coalesced bainite – was found to develop along with the classical martensite, lower and upper bainite.[6] Coalesced bainite develops into a coarse feature through the coalescence of independently nucleated platelets of bainite. This happens when the bainite formation temperature is close to the martensite start temperature.[7] There is evidence that the coarse scale of coalesced bainite is detrimental to the impact toughness.[8] This is because the platelets that coalesce should all be in identical crystallographic orientation and hence create a large region without crystallographic discontinuities, thereby reducing the ability to deflect the propagation of cleavage cracks. To confirm this, it was decided therefore to carry out more fundamental crystallographic studies on coalesced bainite using the combination of FEGSEM and EBSD. The present paper reports on the investigations of this microstructure in different experimental weld metals including comparisons with ordinary lower bainite.

Experimental

Welded joints were made with manual metal arc welding according to ISO2560 using 20 mm plates along with a backing plate (Fig. 1). The joints were first buttered to limit dilution before the deposition of the experimental weld metals which took place in 33 cm runs with two runs per layer and three on the top layer. The welding parameters and chemical compositions are presented in Table 1. The experimental weld metals were designated 7-2L250, 7-0·5L250 and 10-0·5M200; wherein 7 or 10 is the Ni content in wt-%, 2 or 0·5 the Mn content in wt-%, L or M indicates low or medium carbon and 250 or 200 the interpass temperature in °C.

Specimens from the weld metal cross-section were extracted perpendicular to the welding direction, mounted in bakelite, wet ground and polished to 1 μm diamond solution. For LOM or secondary electron imaging with FEGSEM the specimens were etched using 2% nital etchant. A Leitz Aristomet light optical microscope and a Leo Ultra 55 FEGSEM fitted with the HKL Technology EBSD system were used.

[1]Innovation Center, Institution Creganna Medical Devices, Parkmore West, Ballybrit, Galway, Ireland
[2]ESAB Sverige AB, Lindholmsallén 9, 402 77 Göteborg, Sweden
[3]Department of Materials and Metallurgy, University of Cambridge, Pembroke Street, Cambridge CB2 3QZ, UK

*Corresponding author, email endakeehan@hotmail.com

Published by Maney on behalf of the Institute
Received 5 January 2007; accepted 14 February 2007
DOI 10.1179/174328407X226572

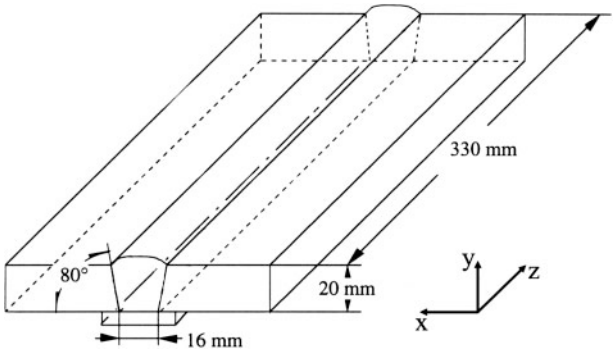

1 Weld geometry along with axis used in EBSD

For EBSD investigations, the specimens were further polished at 0·5 and 0·25 μm diamond solution, which was then followed by polishing with colloidal silica (OPS, Struers) for 15 min. An electron beam of 20 kV was used with a specimen working distance of 15 mm and a specimen tilt angle of 70°. The samples were orientated relative to the EBSD system such that the Z axis was the welding direction; the X axis was the horizontal direction while the Y axis was the perpendicular direction (Fig. 1). Before mapping, the specimens were examined using the forescatter detector, which is part of the HKL EBSD system. This uses diodes to reveal grain and subgrain structure from the sample of interest when it is tilted into the EBSD position. Orientation maps were acquired using a step size of 0·8, 0·2 or 0·15 μm depending on the grain size or the resolution required. In order to achieve good EBSD crystallographic resolution, a step size permitting at least two or three measurements across each grain in any given direction should be chosen. The orientation maps are presented here using the inverse pole figure colouring system. In this, a designated sample axis is plotted relative to crystal axes on a stereographic triangle.[10]

Results

Figure 2 shows lower and coalesced bainite along with martensite in the as deposited last bead of weld metal 10–0·5M200.[11]

Figure 3 shows the y direction orientation map acquired using a step size of 0·8 μm from the as deposited last bead of weld metal 7-0·5L250. The former austenite grains are clearly seen. The transformation of the austenite into a variety of ferritic products divides each grain into crystallographic packets within which the ferrite orientation is uniform. There is structure within each packet but that cannot be identified at the resolution presented.

Table 1 Welding parameters and chemical composition

Weld metal	7-2L250	7-0·5L250	10-0·5M200
E, kJ mm^{-1}	1·2	1·0	1·2
IPT, °C	250	250	200
$t_{8/5}$, s	12	10	9
C	0·032	0·024	0·080
Mn	2·02	0·60	0·56
Ni	7·23	6·60	10·51
Cr	0·47	0·21	1·13
Si	0·25	0·35	0·23
P	0·011	0·01	0·015
Mo	0·63	0·40	0·29
Cu	0·03	0·02	0·30
S	0·008	0·008	0·007
O, ppm	380	400	380
N, ppm	250	197	110

*E is the energy input, IPT the maximum interpass temperature and the estimated cooling time between 800 and 500°C, calculated using WeldCalc is designated $t_{8/5}$ (Ref. 9); composition is in wt-% unless otherwise stated and C, S, O and N are elements analysed using Leco Combustion equipment.

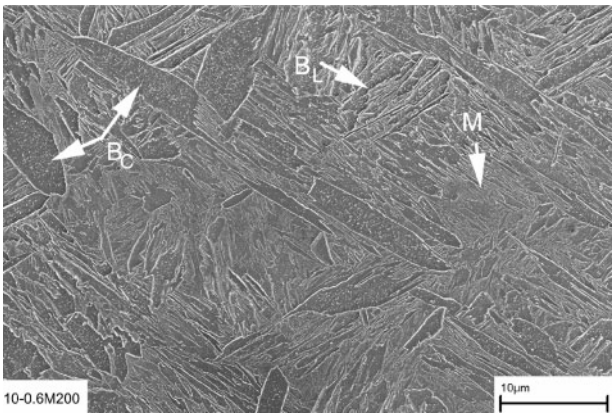

2 Typical morphology of lower and coalesced bainite along with martensite as observed using secondary electrons in FEGSEM, in as deposited last bead of weld metal 10–0·5M200 (Ref. 11)

A crystallographic packet was studied at high magnification in the as deposited bead of weld metal 7-2L250 (Fig. 4). An area containing coalesced bainite along with lower bainite was identified using the forescattered detector (Fig. 4*A*) and an orientation map recorded with a step size of 0·15 μm (Fig. 4*B*).

The boundary of the wedge shaped coalesced bainite grain was examined using a 'point to point' analysis in which the orientation is tracked along a line traversing the interface and the misorientation between adjacent pixels is plotted. All line analyses were made from left to right.

A misorientation of just over 3° was measured between the widest end of the coalesced bainite grain and the surrounding lower bainite (L1, Fig. 4*B*). On moving across the grain with three subsequent line scans, it was found that the grain boundary misorientation with the surrounding bainite increased towards the grain tip (L4).

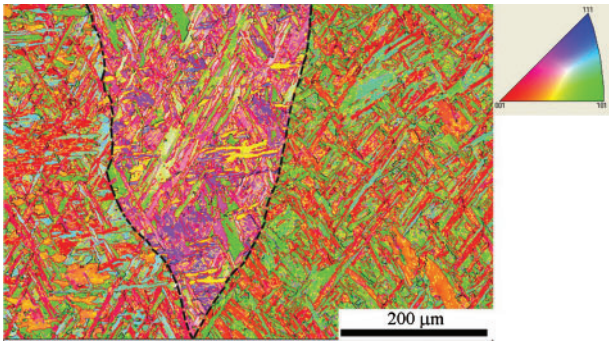

3 Low magnification orientation map using *y* direction inverse pole figure colouring scheme in as deposited last bead of weld metal 7-0·5L250: former austenite grains (broken lines highlight grain boundaries) are made up of many crystallographic packets of transformation products (The full colour version of this paper can be found at www.ingentaconnect.com)

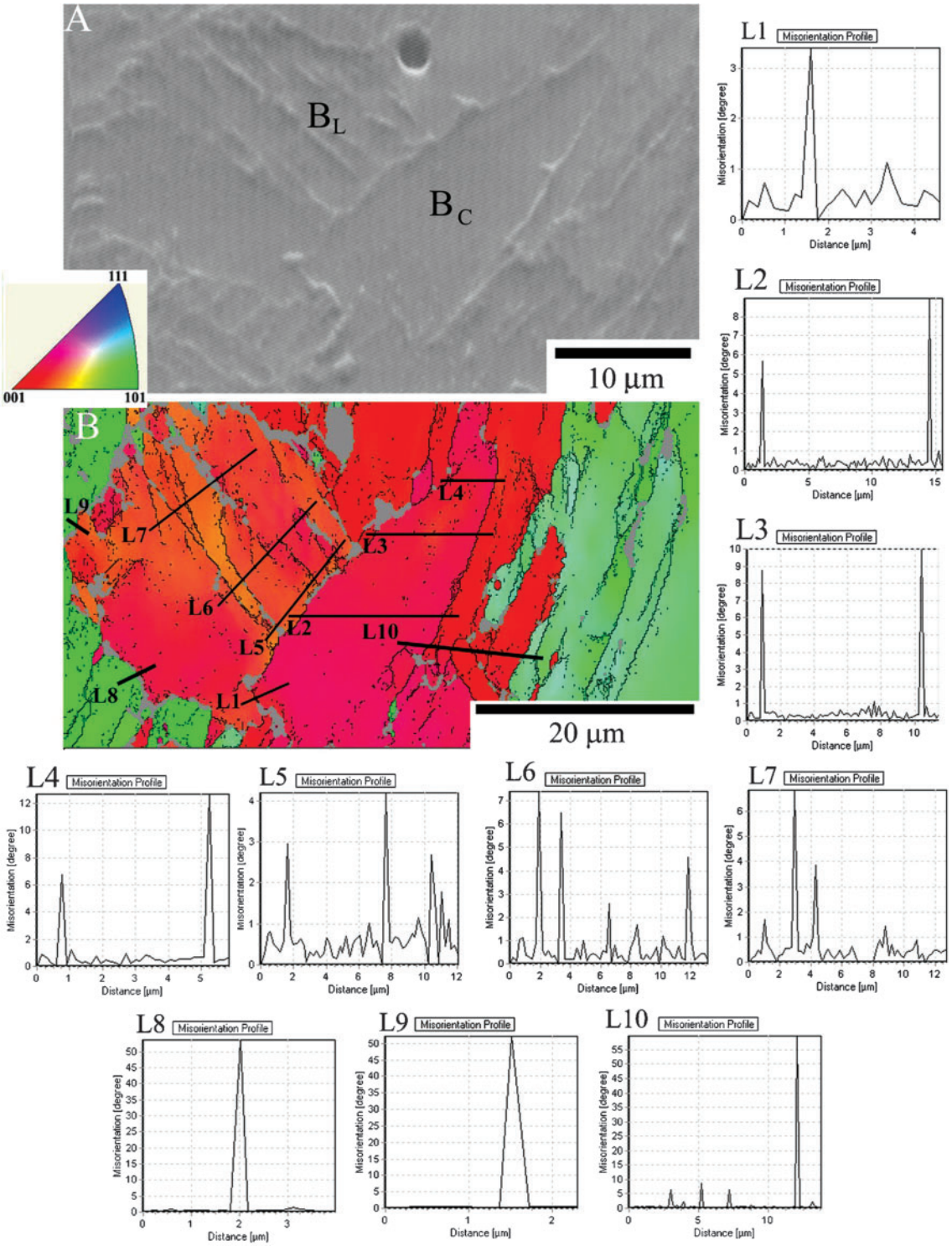

4 ***A*** **image created using forescattered detector system on HKL EBSD system showing large grain of coalesced bainite** B_C **along with lower bainite** B_L **in weld metal 7-2L250 and** ***B*** **corresponding orientation map according to** ***z*** **direction inverse pole figure: four 'point to point' analyses (L1–L4) show misorientation of coalesced bainite relative to surrounding microstructure; scans L5–L7 go across boundaries between different grains of lower bainite and lines L8–L10 illustrate large orientation difference between crystallographic packets (The full colour version of this paper can be found at www.ingentaconnect.com)**

Boundaries between different grains of lower bainite and crystallographic packet boundaries were also examined (L5–L10, Fig. 4). The lower bainite grains were separated by small misorientations between 2 and 8° (L5–L7) whereas packet boundaries (between the red and the green region) exhibited large misorientation angles ranging from 50 to 60° (L8–10).

It is of interest to study the internal crystallography of the coalesced bainite grains as they form by the coalescence of platelets. The grain illustrated in Fig. 4 was therefore examined in more detail, as shown in Fig. 5. Four scans were made across the grain, with the '*A*' diagrams representing point to point orientation differences and the '*B*' diagrams showing the

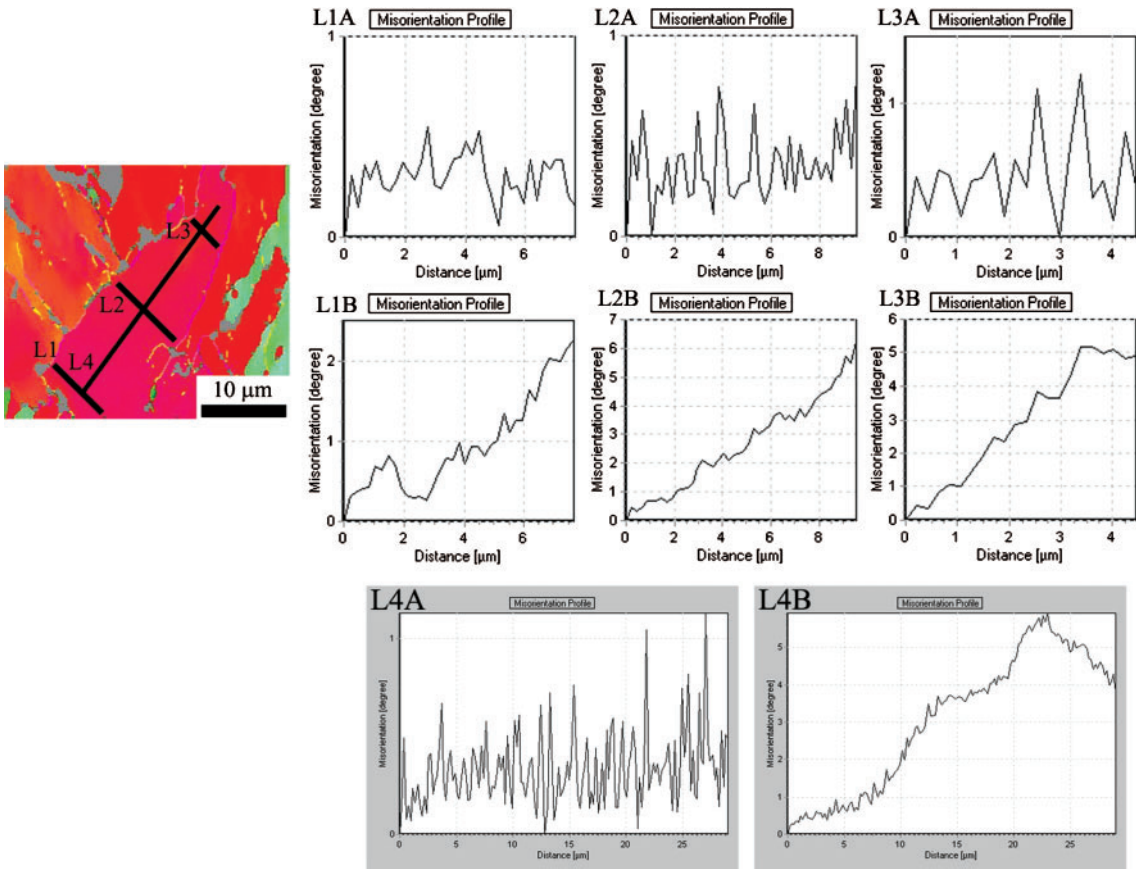

5 Internal crystallography of coalesced bainite grain from weld metal 7-2L250 in Fig. 4. L1A–L4A present point to point misorientation profiles while L1B–L4B present point to origin misorientation with all plot analyses going from left to right

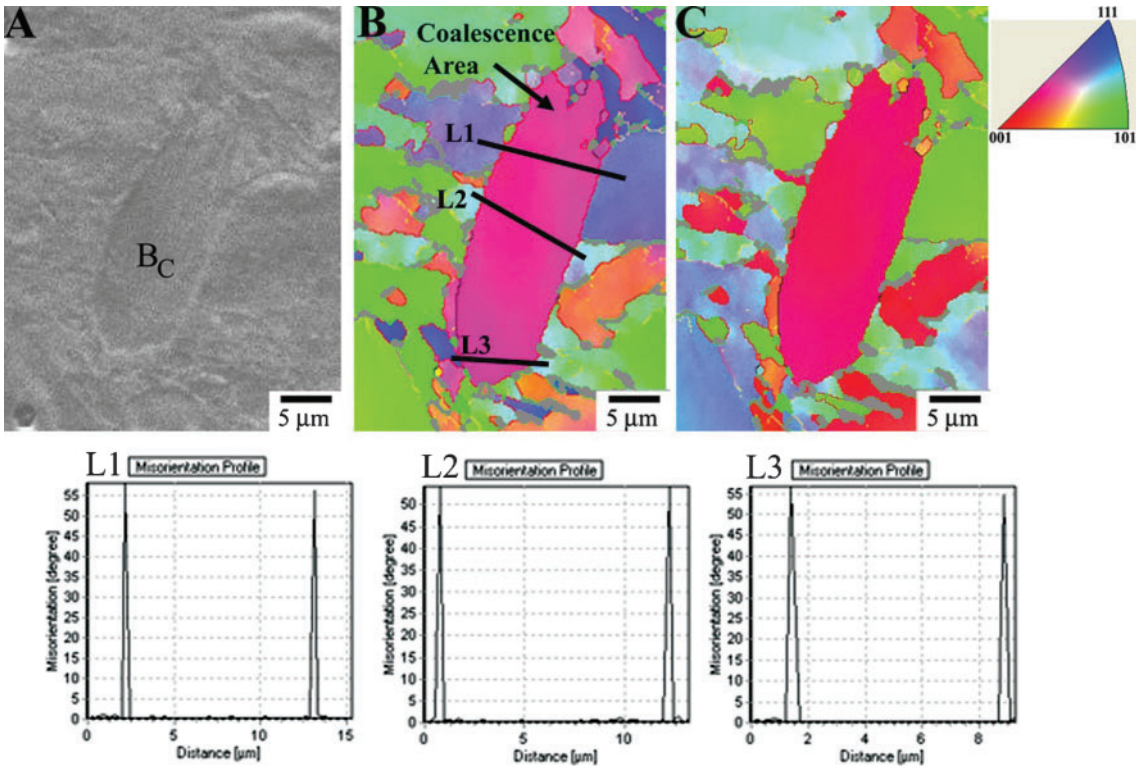

6 *A* forescattered image showing large grain of coalesced bainite B_C in weld metal 10-0·5M200, *B* corresponding orientation map differentiated according to *x* direction inverse pole figure along with *C* y direction orientation map (L1–L3): three line point to point misorientation profiles (going from left to right) that examine grain boundary misorientation between coalesced bainite grain and surrounding microstructure (The full colour version of this paper can be found at www.ingentaconnect.com)

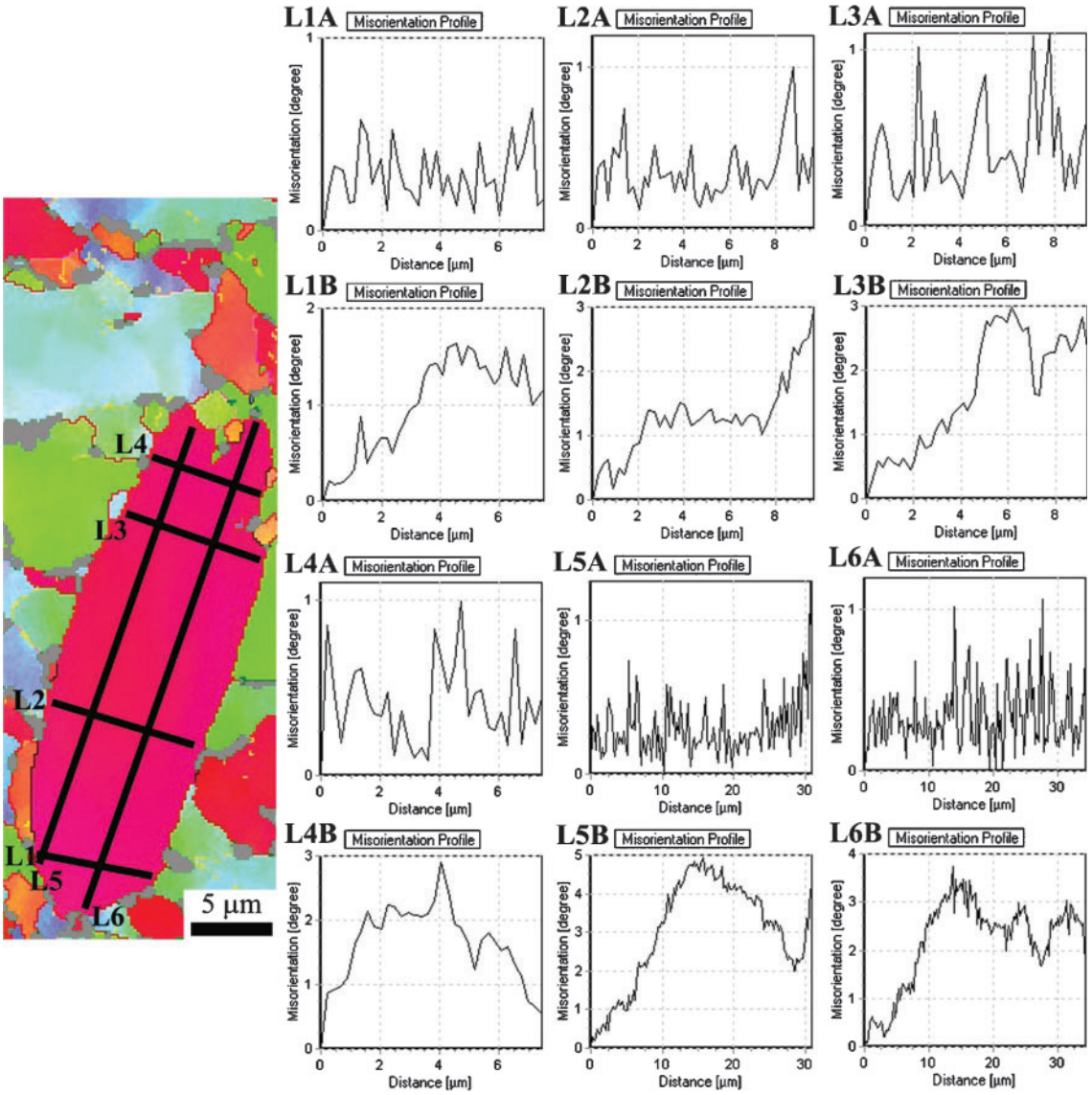

7 Internal crystallography of coalesced bainite grain in weld metal 10-0·5M200 in Fig. 6: L1A–L6A present 'point to point' misorientation profiles while L1B–L6B present 'point to origin' misorientation with analyses going from left to right (The full colour version of this paper can be found at www.ingentaconnect.com)

accumulated point to origin orientation differences. In scans L1A–L4A, it is observed that the local misorientation is generally less than 1°. However, the accumulation of misorientation along and across the grain (L1B–L4B) can be up to 6°.

Coalesced bainite was also studied in weld metal 10-0·5M200. Figure 6 presents a forescattered image of a coalesced bainite grain along with corresponding orientation maps (step size 0·2 μm) shown using x and y direction inverse pole figures. The coalesced bainite grain is particularly prominent in the orientation map. It is crystallographically homogeneous within the limits of the orientation resolution and the maps also expose the area of coalescence clearly where separate parts join together to form one grain. The coalesced grain had large misorientations of between 50 and 60° with the surrounding microstructure (Fig. 6, L1–3) and in this case constitutes an entire crystallographic packet.

The internal crystallography of the coalesced bainite grain (Fig. 6) was also examined (Fig. 7). The results are similar to the coalesced bainite grain examined in Fig. 5 with a misorientation difference up to the region of 1° recorded in point to point investigations and up to 5° recorded in point to origin analysis.

It can be noted that orientation gradients were typically on the order of 3°/10 μm both along and across the grain in Fig. 7 and along the grain in Fig. 5. A similar gradient was measured also across the widest end of the grain in Fig. 5 (line L1) whereas the cross grain gradients at the centre (line L2) and the tip are approximately twice as large with the steepest gradient seen near the tip (line L3).

Discussion

Studies (EBSD) at low magnification require a rather large step size to be used in order to limit the acquisition time length for acquiring the map. In such measurements, information about the former austenite grains and the crystallographic regions they contain is obtained as in Fig. 3. Since the focus of the present work was coalesced bainite, most of the studies were carried out using a small step size (0·2 or 0·15 μm) and higher magnification.

Boundary misorientations

Consistent with previous observations,[12] lower bainite grains are found to be separated by low misorientations (Fig. 4). This was also the case for boundaries between coalesced bainite grains and lower bainite grains belonging to the same crystallographic region (Fig. 4). Much larger orientation differences were found at packet boundaries (Figs. 4 and 6), up to 60°. Large misorientations such as these should strictly be presented as an axis–angle pair, but it is expected that misorientations between crystallographic variants within a given austenite grain can be large.[12]

Coalesced bainite: internal crystallography

The orientation maps show that the large coalesced bainite plates are crystallographically homogeneous (Figs. 4 and 6). On the other hand, there are clear orientation gradients of some 3°/10 μm both along and across the coalesced grains (Figs. 5 and 7). Gradients as large as these cannot be sustained elastically, and hence must be a reflection of plastic relaxation. The strain energy per unit volume of an elastically accommodated plate scales with the thickness to length ratio.[13] The coalescence process must therefore lead to a dramatic increase in the strain energy, which can be reduced by plastic accommodation. The extent of relaxation is likely to be largest in the thicker regions of the plate, whereas elastic accommodation is possible near the tip where the plate is thinner. This is the most likely explanation of the observed orientation gradients and is consistent with the largest gradient observed near the tip of a grain where less plastic accommodation is expected.

Conclusions

Large coalesced bainite grains with many micrometres in length and width appear to be crystallographically homogeneous. Nevertheless, significant misorientation gradients exist within each coalesced grain, probably as a consequence of the plastic accommodation of transformation strains. This is consistent with the fact that coalescence leads to fat plates whose shape deformations are more difficult to accommodate purely elastically within the austenite.

Misorientation studies showed low angle boundaries between neighbouring lower bainite grains and between lower bainite and coalesced bainite grains within a crystallographic packet. Significantly larger orientation differences were found between packet boundaries reflecting differences expected between crystallographic variants of the austenite–ferrite orientation relationship.

Acknowledgements

Mr Johan Elvander, manager of consumable research and development at ESAB AB is thanked for supporting this experimental work and permission to publish results. The microscopy and microanalysis research group within the Department of Applied Physics at Chalmers University of Technology are thanked for use of their instruments.

References

1. L. E. Svensson, J. Elvander and L. Karlsson: *Svetsaren*, 1999, **54**, (1–2), 29–33; Internet: http://www.esab.com/global/en/news/svetsaren.cfm
2. D. J. Widgery: 'High strength weld metals – Routes for development', IIW Document II-A-098-02.
3. D. J. Widgery, L. Karlsson, M. Murugananth and E. Keehan: Proc. 2nd Int. Symp. on 'High strength steel', Stiklestad, Verdal, Norway, April 2002, European Coal and Steel Community (ECSC), B-1049.
4. E. Keehan, L. Karlsson, M. Thuvander and E. L. Bergquist: 'Microstructural characterisation of as-deposited and reheated weld metal – high strength steel weld metals', IIW Doc. IX-2187-06, 2006.
5. A. F. Gourgues, H. M. Flower and T. C. Lindley: *Mater. Sci. Technol.*, 2000, **16**, (1), 26–40.
6. E. Keehan, L. Karlsson and H. O. Andrén: *Sci. Technol. Weld. Join.*, 2006, **11**, 1–8.
7. L. C. Chang and H. K. D. H. Bhadeshia: *Mater. Sci. Technol.*, 1996, **12**, (3), 233–236.
8. E. Keehan, L. Karlsson and H. O. Andrén: *Sci. Technol. Weld. Join.*, 2006, **11**, 9–18.
9. SSAB: WeldCalc, 1998–1999, Oxelösund, Sweden.
10. A. J. Schwartz, M. Kumar and B. L. Adams (eds.): 'Electron backscatter diffraction in materials science'; 2000, New York, Kluwer Academic/Plenum.
11. E. Keehan, L. Karlsson, H. O. Andrén and H. K. D. H. Bhadeshia: Proc. Int. Conf. on 'Trends in welding research', 2005, Alanta, GE, ASM International.
12. J. R. Yang and H. K. D. H. Bhadeshia: *Mater. Sci. Technol.*, 1989, **5**, (1), 93–97.
13. H. K. D. H. Bhadeshia, E. Keehanz, L. Karlssonz and H. O. Andren: *Trans. Ind. Inst. Met.*, 2006, **59**, 689–694.